Environmental Engineering and Management Journal *August 2014, Vol.13, No. 8, 1987-1995*
http://omicron.ch.tuiasi.ro/EEMJ/

"Gheorghe Asachi" Technical University of Iasi, Romania

ELECTROCHEMICAL PROPERTIES OF FLUORINATED HYDRAZINO-PYRAZOLES IN [BMIM$^+$][BF_4^-] IONIC LIQUID

Liviu-Virgil Costea[1*], Günter Fafilek[2], Hermann Kronberger[2]

[1]*University "Politehnica" Timişoara, Faculty of Industrial Chemistry and Environmental Engineering, Bd. Vasile Pârvan, nr. 6, 300223, Timişoara, Romania;*
[2]*Vienna University of Technology, Faculty of Technical Chemistry, Institute of Chemical Technologies and Analytics, Getreidemarkt 9, 1060 Wien, Austria*

Abstract

The electrochemical properties of two fluorinated substrates, namely 1H-3-methyl-4-ethoxycarbonyl-5-(4-fluoro-benzylidenehydrazino)-pyrazole (Ia) and 1H-3-methyl-4-ethoxycarbonyl-5-(2-fluoro-benzylidenehydrazino)-pyrazole (Ib) respectively have been investigated in the room temperature ionic liquid (RTIL) 1-butyl-3-methylimidazolium tetrafluoroborate on a platinum electrode. The voltammetric investigation of the above compounds in the mentioned RTIL shows mainly two irreversible anodic peaks on a wide range of scan rates. Mechanistic studies involving the estimation of the diffusion coefficient, number of transferred electrons in the rate-determining step as well as charge transfer coefficients show that the main aspects of the anodic oxidation of the given substrates follows an EC mechanism which is similar to that observed in molecular solvents leading to the assumption that oxidative ring closure reactions may be conducted in RTILs as well, providing a starting point in finding a new more sustainable method of obtaining the latter compound. The aim of the present work is to extend the current findings gathered previously in order to find a more environmentally friendly and sustainable way of obtaining various pyrazolo-triazoles.

Key words: anodic oxidation, ionic liquid, pyrazole, pyrazolo-triazole

Received: February, 2014; Revised final: August, 2014; Accepted: August, 2014

1. Introduction

In recent years, the concept of green and sustainable chemistry has become even more a topic of interest, focusing mainly on finding reaction patterns and ways of developing certain synthesis paths that generate less by-products with lower energy consumption and thus a lighter impact on the environment (Doble and Kruthiventi, 2007). In a broader perspective new processes have to be developed, that minimize the use of hazardous materials as well as the quantity of toxic waste. They have to be more energy efficient and make better use of renewable reaction media.

Electrochemical techniques have attracted much attention in the last decade proving that they can provide an extremely versatile way to selectively reduce and/or oxidize organic compounds, thus being an important tool in designing new sustainable synthetic pathways (Brillas and Siré, 2011; Fotouhi et al., 2006).

The scientific interest towards nitrogen containing heterocycles and especially pyrazolo-triazoles lies mainly in their use as precursors in various organic syntheses (Bailey, 1977) and their biological and pharmacological activities (Bansal and Thota, 2013; Iradyan et al., 2011; Rollas and Küçükgüzel, 2007). This class of compounds finds its use as precursors in obtaining color photosensitive materials (Bailey et al., 1967; Diehl et al., 2000) as well as inks and toners (Tatsuo et al., 1998).

1H-3-methyl-4-ethoxycarbonyl-5-substituted-benzylidene-hydrazino-pyrazoles (**I**) are an important class of starting materials in obtaining various

∗ Author to whom all correspondence should be addressed: e-mail: livius.costea@gmail.com

heterocyclic systems including the 1H-3-aryl-7-ethoxycarbonyl-6-methyl-pyrazolo[5,1-c][1,2,4]triazoles (**II**) (Fig. 1).

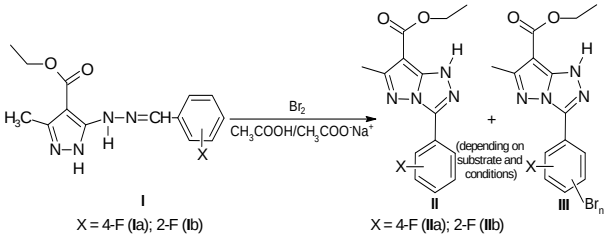

Fig. 1. Chemical cyclization pathways of 1H-3-methyl-4-ethoxycarbonyl-5-substituted-benzylidene-hydrazino-pyrazoles (**I**) in the presence of bromine/glacial acetic acid

Depending on the nature of the substituents grafted on the benzene ring and the specific working conditions, one can obtain the desired cyclization product (II) or the corresponding brominated compound (III) (Bailey, 1977; Bercean, 1988; Bercean et al., 2005). In order to avoid the use of hazardous chemicals like bromine or lead tetraacetate during the process and to find a more sustainable way in obtaining compound **II**, our previous studies were mainly focused on elucidating the reaction mechanism governing the anodic oxidation of various substrates of type **I** in nonaqoueous aprotic solvents in order to find new, more reliable ways of obtaining pyrazolo-triazoles (**II**) by means of electro-synthesis (Costea et al., 2006a, b; Costea et al., 2008). In the present study we employed ionic liquids as a new reaction environment for voltammetric studies in our quest for an environmentally friendly alternative to organic molecular solvents.

Ionic liquids (ILs) represent a broad class of salts which melt at or below 100^0C. Room temperature ionic liquids (RTILs) in turn, are a subset of ionic liquids that are in a liquid state at room temperature. The remarkable properties of these compounds rely on the fact that they are composed entirely of ions. As a result, RTILs may behave quite differently from common molecular solvents when used as reaction media (Sun and Armstrong, 2010). The use of RTILs in the field of electrochemistry is mostly driven by their high conductance (which, in most cases makes the use of supporting electrolyte completely unnecessary), extended electrochemical window as well as their high chemical stability, low volatility and low or extremely low vapor pressure (Kerton, 2009; Wagner et al., 2010).

Based on the promising results regarding the anodic cyclization of 1H-3-aryl-6-methyl-7-ethoxycarbonyl-pyrazolo[5,1-c][1,2,4] triazoles and 1H - 3 - Methyl - 4 - ethoxycarbonyl - 5 - (4 - fluoro - benzylidenehydrazino) - pyrazole respectively (Costea et al., 2006a, b; 2009), we intended to further investigate the possibility of conducting the above mentioned process in the room temperature ionic liquid (RTIL) 1-butyl-3-methylimidazolium tetrafluoroborate ($BMIMBF_4$), applying the principles of "green chemistry".

We've studied the electrochemical properties of the hydrazones **I**a and **I**b (Scheme 1) substituted with -F in nonaqueous acetonitrile (ACN) and compared them to the electrochemical behavior of the latter substrates in the mentioned RTIL. Because, to our knowledge, the scientific literature covering this issue is rather scarce we hereby firstly present the electrochemical behavior of substrates **I**a and **I**b in the RTIL 1-butyl-3-methylimidazolium tetrafluoroborate. The aim of the present work is to extend the current findings previously gathered in order to find a more sustainable way of obtaining various pyrazolo-triazoles by avoiding the use of toxic organic solvents as well as hazardous oxidation agents.

2. Experimental

2.1. Chemicals

1H - 3 - Methyl - 4 - ethoxycarbonyl - 5 - (4 - fluoro - benzylidenehydrazino) - pyrazole, (**I**a, X = 4 - F), 1H - 3 - Methyl - 4 - ethoxycarbonyl - 5 - (2 - fluoro - benzylidenehydrazino) - pyrazole, (**I**b, X = 2 - F) and 1H - 3 - (2 - fluoro - phenyl) - 6 - methyl - 7 - ethoxycarbonyl - pyrazolo [5, 1 - c][1, 3, 4] triazole (**II**b, X = 2 - F) were obtained according to the literature (Bailey et al., 1967; Bercean, 1988; Bercean, et al., 2005).

Anhydrous acetonitrile (ACN), analytical grade (Aldrich) containing less than 0,001% water and 1-Butyl-3-methylimidazolium tetrafluoroborate ($BMIMBF_4$) (Merck, high purity) were stored under inert nitrogen atmosphere and molecular sieves and were used as purchased. Ferrocene (Aldrich), used as an internal reference for calibrating electrode potentials was also used as purchased.

Thin layer chromatography was performed using 60F254 silica gel plates (Merck) and a mixture of benzene: ethyl acetate = 1:1 as eluant. Melting points were recorded with a Boetius PHMK (Veb–Analytik Dresden) apparatus. As determined by HPLC, the studied substrates show a purity of >99%. HPLC analyses were conducted with a Merck Chromolith Performance 2 column, using acetonitrile/H_2O as eluant. IR spectra were recorded with a JascoFT/IR-410 Infrared Spectrophotometer using KBr disks and Bruker Avance 300 spectrometers were used for 1H-NMR and 13C-NMR spectroscopy.

2.2. Cyclic voltammetry experiments

The study of the electrochemical properties of the benzylidenehydrazino - pyrazole **I**a and **I**b and the pyrazolo - triazole **II**b was conducted by recording the cyclic voltammograms over the potential range of interest in the given reaction medium. Cyclic voltammetry experiments were performed using a Jaissle 1200PCT potentiostat/

galvanostat, coupled to an Agilent 33120 A signal generator and an Agilent 34970-A data acquisition system using Pt-disk working and Pt-wire auxiliary electrodes at room temperature. A custom-made three electrode cell with a Teflon cap tailored to house the electrodes and the gas inlet, containing 7 mL solution was employed for the electrochemical measurements.

The solvent-supporting electrolyte system consisted of dry acetonitrile and tetra-n-butylammonium tetrafluoroborate (Aldrich, for electrochmistry) or 1-Butyl-3-methylimidazolium tetrafluoroborate with no further electrolyte added. Stock solutions of the studied substrates in CH_2Cl_2 were prepared and a certain amount was introduced into the electrochemical cell containing $BMIMBF_4$ using a micropipette. Dry nitrogen was then bubbled through the IL for at least 1 hour in order to evaporate the latter solvent. Solutions for all voltammetric analyses were deoxygenated with nitrogen dried over a column of molecular sieves and kept under an inert atmosphere throughout the experiments. The reference electrode for the experiments conducted in the RTIL consisted of a Pt wire immersed in $BMIMBF_4$ separated from the bulk solution by a frit. This reference showed a stable potential towards the ferrocene/ferricinium (Fc/Fc^+) couple for more than 48h. Ferrocene was added to the electrolyte solution at the final stage of each measurement, the Fc/Fc^+ couple acting as an internal standard. All potentials are mentioned with reference to the Fc/Fc^+ couple.

3. Results and discussion

3.1. Cyclic voltammetry in acetonitrile

The anodic oxidation of the benzylidenehydrazino-pyrazoles **I**a and **I**b in dry acetonitrile was investigated by cyclic voltammetry. Earlier results based on studies concerning the anodic oxidation of benzylidenehydrazino - pyrazole **I**a in nonaqoueous aprotic solvents like acetonitrile and DMSO respectively (Costea et al., 2006a, b; 2009) showed that the substrate undergoes an initial electron transfer step, the positive reaction center herein formed being strongly influenced by the substituents grafted on the para position of the outer benzene ring.

The cyclic voltammetric response of substrate **I**a in acetonitrile on a Pt working electrode at sweep rates varying from 20 to 1000 mVs^{-1} is shown in Fig. 2. The benzylidenehydrazino - pyrazole **I**a exhibits two very well defined oxidation peaks at potentials of 1.085 and 1.750 V respectively at a scan rate of 50 mVs^{-1}. Before the second peak arises, a shoulder or pre-peak is observed but only at relatively slow sweep rates, completely disappearing when scanning above 100 $mV{\cdot}s^{-1}$. The chemical irreversibility of the two peaks is sustained by the fact that even at high scan rates no reverse reduction peak is observed corresponding to the mentioned oxidation signals. The analysis of the first anodic wave according to the established electrochemical criteria allows a more detailed understanding of the charge transfer steps involved (Cekic-Laskovic et al., 2009). The plot of the logarithm of the peak current recorded for the first wave against the logarithm of the scan rate is clearly a straight line, indicating that this wave corresponds to a diffusion controlled process. The slope of about 0.45 for the first peak and 0.56 for the second differs slightly from the theoretical value of 0.5 indicating a certain influence of the adsorbed intermediates at the electrode surface (Laviron, 1980). The peak potential, Ep was found to increase linearly with respect to the logarithm of the scan rate for both peaks having a slope of 21 and 31 mV, respectively, in accordance with a totally irreversible oxidation process (Fig. 3 inset) (Pletcher et al., 2002).

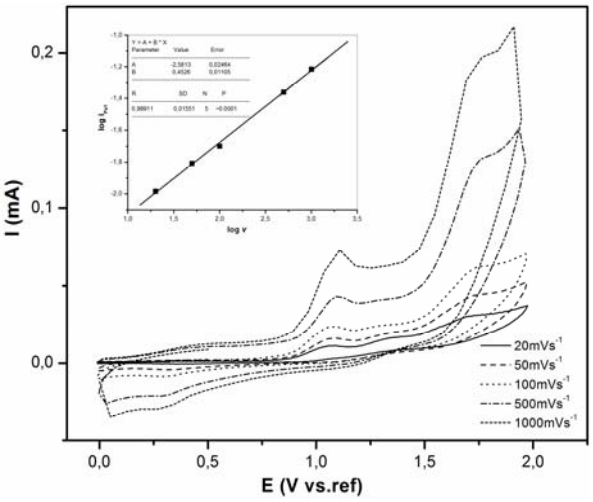

Fig. 2. Cyclic voltammogram of **I**a in anhydrous acetonitrile. Conditions: substrate concentration, $c=2{\cdot}10^{-3}$ $mol{\cdot}dm^{-3}$; supporting electrolyte: $c=0.1$ $mol{\cdot}dm^{-3}$ tetra-n-butyl ammonium tetrafluororborate; working electrode: Pt; auxiliary electrode: Pt wire; reference electrode: Ag/AgCl; scan rate $20{\cdot}10^{-3}$ - $1000{\cdot}10^{-3}$ $V{\cdot}s^{-1}$.
Inset: plot of log(i) vs. log (v) for the first oxidation wave at the mentioned scan rates

The current function $Ip{\cdot}v^{1/2}$ decreases exponentially with increasing scan rate for both oxidation peaks (Fig. 2) as an indication of either, a reversible or irreversible charge transfer step followed by a homogenous chemical reaction (Nicholson and Shain, 1964). All the data presented above, along with the characteristic shape of the voltammograms recorded for the oxidative region (Fig. 2) lead us towards the assumption that the process follows a two-step EC mechanism with a reaction pattern involving the subsequent deprotonation of the initially formed cation radical as the most probable first homogenous reaction step.

The electrochemical behavior of substrate **I**b in acetonitrile on a Pt working electrode at sweep rates varying from 20 to 1000 mVs^{-1} has been studied in order to elucidate whether the substituent grafted on the ortho position of the benzene ring could have a significant influence on the reaction center eventually hindering the formation of the

intermediate cation radical. The substrate **I**b has a fairly similar behavior compared to the latter, except for the shape of the first oxidation peak which tends to be extremely broad and ill-defined at higher sweep rates. The first oxidation peak at 1.110 V at v = 50 $mV \cdot s^{-1}$ has slightly shifted towards a more positive potential as an indication of more energy being needed to form the intermediate.

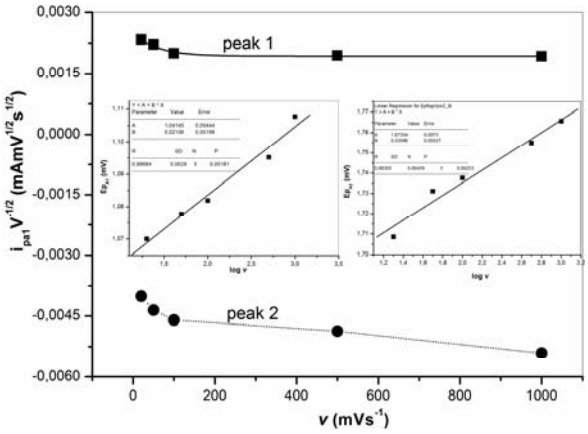

Fig. 3. Variation of the current function $ip_a \cdot v^{1/2}$ for both oxidation peaks of compound **I**a in acetonitrile for various scan rates. Inset: Dependence of the peak potential on the logarithm of scan rate for both oxidation waves of compound **I**a

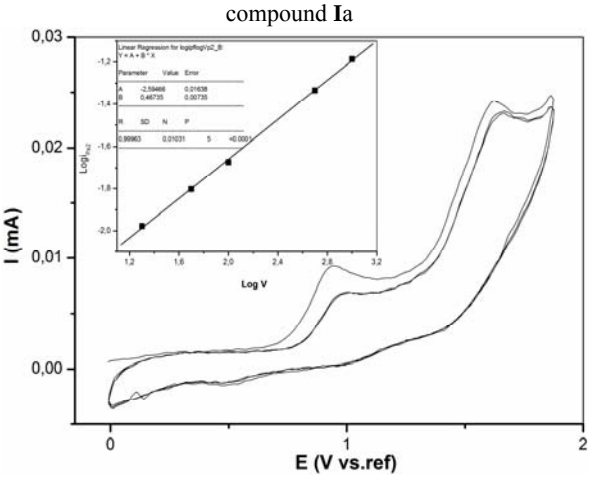

Fig. 4. Multisweep cyclic voltammogram of **I**b in anhydrous acetonitrile. Conditions: substrate concentration, $c=2 \cdot 10^{-3}$ $mol \cdot dm^{-3}$; supporting electrolyte: $c=0.1$ $mol \cdot dm^{-3}$ tetra-n-butyl ammonium tetrafluororborate; working electrode: Pt; auxiliary electrode: Pt wire; reference electrode: Ag/AgCl; scan rate $50 \cdot 10^{-3} V \cdot s^{-1}$. Inset: plot of log(i) vs. log (v) corresponding to the first oxidation wave of compound **I**b

The second peak at 1.670 V is an indication of a more unstable intermediate formed during the first charge transfer step of this substrate. In order to clarify the possible adsorption complications that may occur at the electrode we conducted a multi-cyclic voltammogram (Fig. 4) at a sweep rate of 50 $mV \cdot s^{-1}$. A significant decrease in peak current after the first scan along with a shift towards a more positive peak potential with succeeding potential scans as well as a slope of 0.82 of the log(i)-log(v) dependence (data not shown) suggests the involvement of adsorbed species at the electrode during this step (Gösser, 1993). The second oxidation peak is well defined and shifts very little towards more positive potentials during the successive scans. The plot of log(i) vs. log(v) for this peak is 0.47 close to the theoretical value, indicating a mainly diffusion controlled process.

As expected, Ep was found to increase linearly with respect to the logarithm of the scan rate for both peaks having a slope of 135 and 76 mV, respectively following the characteristics of a totally irreversible oxidation system (Fig. 5 inset) (Pletcher et al., 2002) but the higher slope found for the first oxidation peak may be due to the adsorption complications mentioned above. Like in the case of substrate **I**a the current function $Ip \cdot v^{1/2}$ decreases exponentially with increasing scan rate (Fig. 5) as an indication of either, a reversible or irreversible charge transfer step followed by a homogenous chemical reaction or even adsorption phenomena (Nicholson and Shain, 1964).

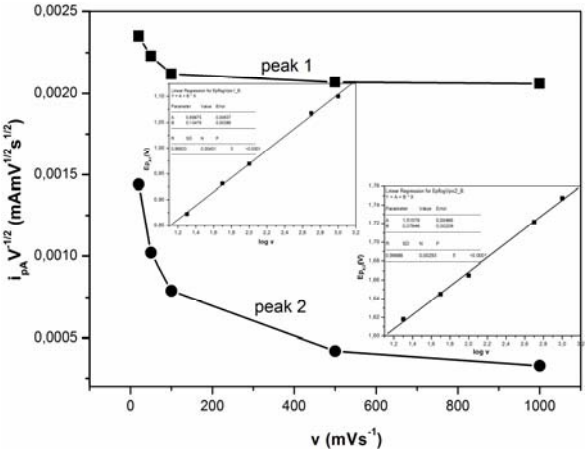

Fig. 5. Variation of the current function $ip_a \cdot v^{1/2}$ for both oxidation peaks of compound **I**b in acetonitrile for various scan rates. Inset: Dependence of the peak potential on the logarithm of scan rate for both oxidation waves of compound **I**b

3.2. Cyclic voltammetry in $BMIMBF_4$

Room temperature ionic liquids being composed entirely of ions may change the electrochemical behavior of substrates formerly investigated in aprotic solvents. In order to find out if these new solvents could be suitable for the anodic cyclization of hydrazones **I**a and **I**b respectively, we have investigated the latter substrates in $BMIMBF_4$ by cyclic voltammetry. Fig.6 shows the cyclic voltammogram of compound **I**a at sweep rates ranging between 10 and 500 $mV \cdot s^{-1}$.

The shapes of the voltammograms recorded in the ionic liquid $BMIMBF_4$ do not differ fundamentally from those obtained in dry ACN, showing two well defined peaks at about 0.98 V and 1.60 V respectively (at a scan rate v = 50 $mV \cdot s^{-1}$). No corresponding reduction peaks occur, even at higher

scan rates suggesting that the oxidation of **I**a in the ionic liquid medium consists of a heterogeneous charge transfer followed by a chemically irreversible process. The positively charged intermediate generated at the electrode is most probably undergoing a fast homogenous transformation, albeit being depleted from the electrical double layer before reduction can occur.

The shoulder observed between the two anodic signals recorded in ACN does not appear under these conditions. It is worth mentioning that, by increasing the scan rate the height of the first oxidation signal is decreasing, the peak disappearing completely at sweep rates higher than 500 mV·s^{-1}. To our assumption this behavior may rely on the slow charge transfer kinetics of the first oxidation step. The high viscosity of the used ionic liquid $BMIMBF_4$, may lead to relatively low diffusion coefficients (Lagrost et al., 2005) which in turn affects the overall oxidation process, meaning that, at high sweep rates, substrate can hardly reach the electrode surface to initiate charge transfer whithin the timescale of the experiment. The effects of ion pairing, reported to most likely occur in ionic liquids (Hollóczki et al., 2014) may lead to a further stabilization by tetrafluoroborate anions, of the radical cation formed after the first oxidation step (Bhat and Ingole, 2012).

In order to investigate the above mentioned feature, we recorded the voltammetric response of **I**a varying the sweep rate by the same increment but switching the potential shortly after the first anodic peak (Fig. 6 Inset). The signal seemed to be well defined even at high scan rates and no reverse peak was observed. In order to get a clearer picture of the processes under investigation the known diagnostic criteria where applied.

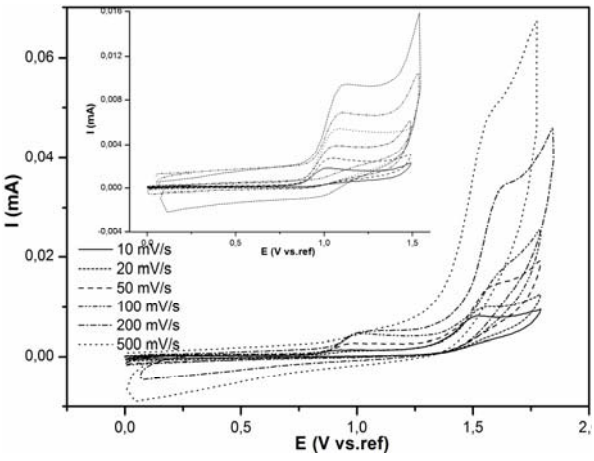

Fig. 6. Cyclic voltammogram of **I**a in $BMIMBF_4$. Conditions: substrate concentration, c=8·10^{-3} mol·dm^{-3}; working electrode: Pt; auxiliary electrode: Pt wire; reference electrode: Pt/RTIL; scan rate 10·10^{-3} - 500·10^{-3} V·s^{-1}. Inset: Cyclic voltammogram of **I**a under the same conditions, potential reversed after the first oxidation peak

For a diffusion controlled electrode process, the peak current Ip is directly proportional to the square root of the scan rate $(v)^{1/2}$, resulting in a straight line when plotted (Brett and Brett, 1994). Adsorption of the electroactive species would result in a linear plot of Ip vs. v. Scanning towards oxidative potentials up to a switching potential of Es = 1.5 V at sweep rates between 10 and 500 mV·s^{-1} while keeping the experimental conditions unchanged gave a linear dependence of the peak current with respect to the root of the scan rate showing an intercept of nearly zero current. These findings suggest that the first anodic peak of the hydrazone **I**a is mainly diffusion controlled (Fig. 7). The variation of the logarithm of the peak current of the first anodic wave against the logarithm of the scan rate is a straight line with a slope of about 0.44 (Fig. 7 inset) being an indication for a diffusion controlled process with some minor adsorption complications (Laviron, 1980).

We have analyzed the electrode process corresponding to the first oxidation wave in terms of variation of the peak current normalized by the square root of scan rate (current function) and the dependence of peak potential to the logarithm of scan rate. Whereas the current function was exponentially decaying with higher sweep rates (Fig. 8) as an indication of an electron transfer step followed by a chemical reaction (case VII of the Nicholson-Shain criteria), the peak potential, Ep_{A1} was found to increase linearly with respect to the logarithm of the scan rate. The slope of 66 mV is in accordance with the case of a chemically irreversible anodic oxidation (Fig. 8 inset) (Pletcher et al., 2002).

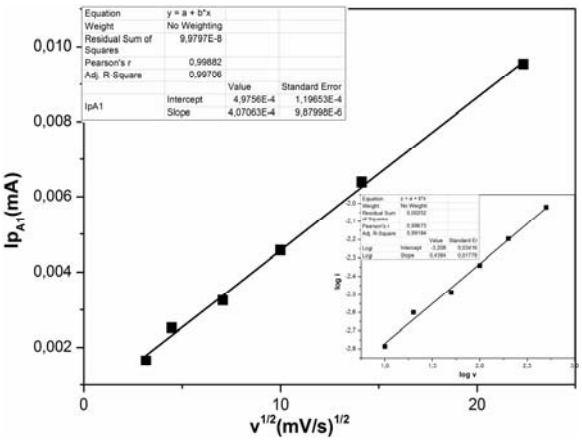

Fig. 7. Plot of the peak current of substrate **I**a for the first oxidation peak versus the square root of the scan rate. Inset: Plot of log(i) vs. log (v) for the first oxidation wave of substrate **I**a

Compound **I**b was also analyzed by cyclic voltammetry in the ionic liquid $BMIMBF_4$ in order to find out if the latter could act as a suitable reaction medium for the anodic cyclization of the studied hydrazone. A typical electrochemical response of **I**b in the RTIL is shown in Fig. 9. The electrochemical behavior seems to be quite similar to the one recorded in ACN regarding the fact that the oxidation peaks have no cathodic counterparts, that being the

first clue upon suggesting an irreversible system. The first oxidation peak, at a sweep rate of 100 mV·s^{-1}, occurs at a potential of about 1.02 V. The value is slightly more positive than the one seen in **I**a, as expected taking into account that the F atom grafted on the para position might stabilize the radical cation formed after the first step (Costea et al., 2006b). The second peak, at about 1.70 V is again shifted to more positive values, due to inductive effects or steric hindrance of the positive reaction center.

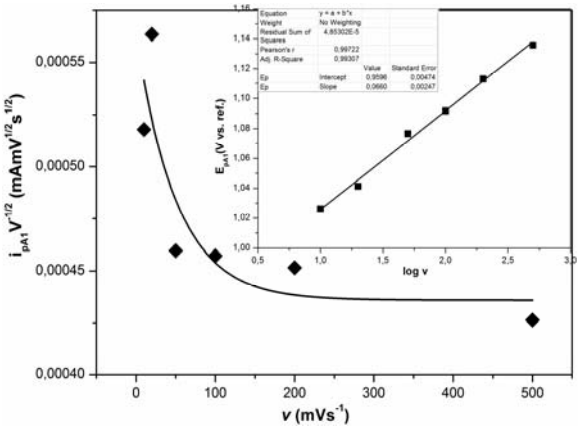

Fig. 8. Variation of the current function $ip_a \cdot v^{1/2}$ for the first oxidation peak of compound **I**a in $BMIMBF_4$ for various scan rates. Inset: Dependence of the peak potential on the logarithm of scan rate for the first oxidation wave of compound **I**a

There is a notable difference between the signals recorded in ACN and those in the RTIL, namely the occurrence of a third broad peak at a potential of about 1.98 V. This signal might be attributed to the pyrazolo-triazole formed after the intramolecular cyclization (Costea et al., 2006a). When setting the switching potential at 1.5 V, only the first oxidation peak occurs, with no reduction counterpart (Fig. 9, continuous line).

Applying the above mentioned criteria for the first oxidation peak, we found that the plot of Ip versus the square root of the scan rate $(v)^{1/2}$ yields a straight line (Fig. 9 inset A) with an intercept of 0.0123, very close to the theoretical value while the plot of log(i) vs. log(v) had a slope of 0.33 indicating an important influence of adsorbed electroactive species at the electrode surface.

The first oxidation wave of compound **I**b was analyzed in terms of the variation of the peak current normalized by the square root of scan rate (current function) with scan rate and the dependence of peak potential to the logarithm of scan rate. As in compound **I**a, the current function was exponentially decaying with higher sweep rates (Fig. 10) as an indication of an electron transfer step followed by a chemical reaction but the much lower peak currents account for a slow charge transfer process or complications due to low diffusion coefficients in the more viscous RTIL.

The peak potential was also found to increase linearly with respect to the logarithm of the scan rate, the slope of about 55 mV, lower as in compound **I**a is in accordance with a chemically irreversible anodic oxidation (Fig. 10 Inset) (Pletcher et al., 2002).

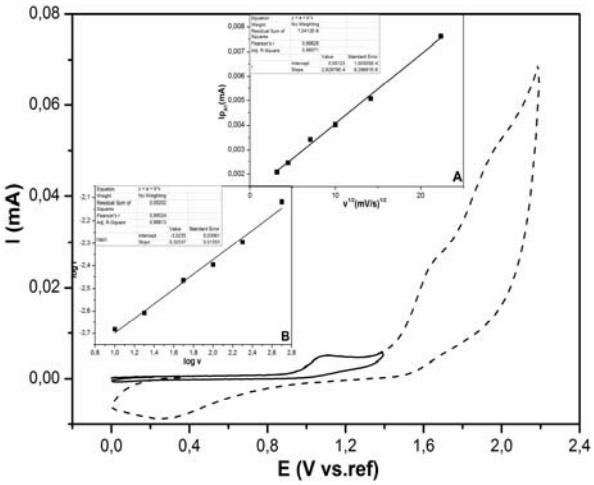

Fig. 9. Cyclic voltammogram of **I**b in $BMIMBF_4$. Conditions: substrate concentration, c=8·10^{-3} mol·dm^{-3}; working electrode: Pt; auxiliary electrode: Pt wire; reference electrode: Pt/RTIL; scan rate 100·10^{-3} V·s^{-1}. Inset: (A) Plot of the electrocatalytic current for the first anodic peak versus the square root of the scan rate for compound **I**b; (B) Plot of log(i) vs. log(v) for the first oxidation wave of compound **I**b

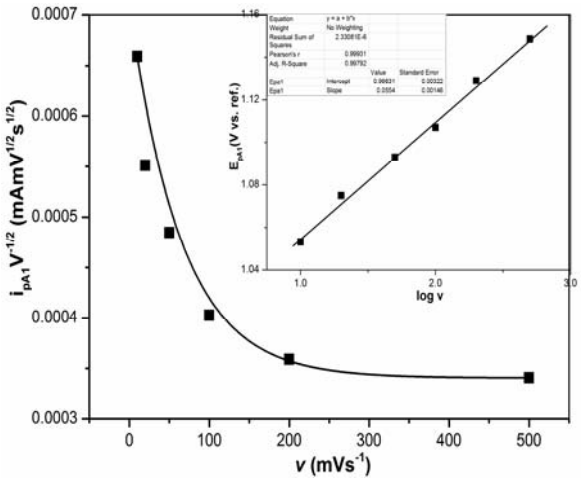

Fig. 10. Variation of the current function $ip_a \cdot v^{1/2}$ for the first oxidation peak of compound **I**b in $BMIMBF_4$ for various scan rates. Inset: Dependence of the peak potential on the logarithm of scan rate for the first oxidation wave of compound **I**b

So far we have arguments to state that the first oxidation wave of both substrates **I**a and **I**b in RTIL medium is characteristic for a slow charge transfer followed by a chemically irreversible process (EC-type mechanism) in which the electroactive species might be weakly adsorbed at the electrode. The high viscosity of the solvent has an impact on the recorded voltammetric waves by retarding the mass transport to the electrode.

A difference worth mentioning is the fact that compound **I**b displays a third peak in the potentiodynamic curve. This behavior might occur

due to the poorer stabilization of the radical cation intermediate formed after the first oxidation wave of **I**b, making the subsequent homogenous reaction to occur faster on the timescale of the experiment. Recent reports suggest that in the present reaction medium the anion of the RTIL, namely $[BF_4]^-$ might play an important role in the overall electrode process by reacting with the protons to form HBF_4 and that the formed acid decomposes to HF and BF_3 (Barnes et al., 2010).

The data presented above, corroborated with the analysis of the starting compounds in anhydrous ACN come to sustain our previous studies in the field that revealed a direct conjugation of the substituents attached to the outer phenyl ring with the positive reaction center and the extended charge delocalization on the molecular orbitals of the corresponding radical cations. Costea et al. (2006a) lead us to propose the following ECEC type reaction mechanism of substrates **I**a and **I**b substituted with -F on the outer benzene ring (Fig. 11):

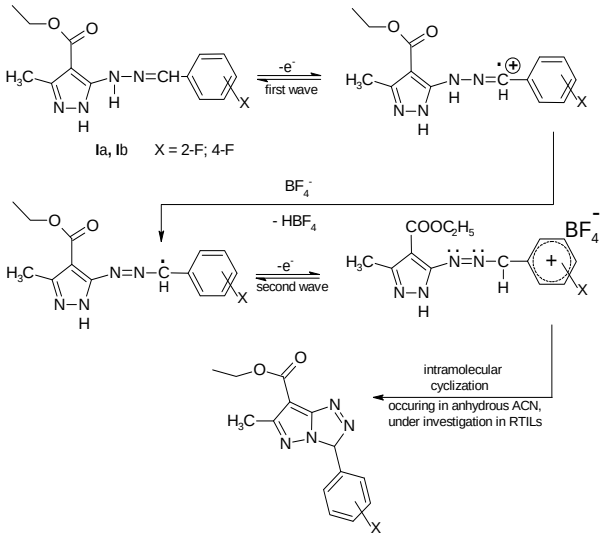

Fig. 11. Suggested reaction mechanism for the anodic oxidation of the 1H-3-methyl-4-ethoxycarbonyl-5-substituted-benzylidene-hydrazino-pyrazoles **I**a and **I**b in $BMIMBF_4$

In order to get a better insight into the first step of the heterogenous charge transfer, the symmetry factors (charge transfer coefficients α) in $BMIMBF_4$ were evaluated. For a more accurate estimation we calculated the values of the charge transfer coefficients for both substrates by three independent approaches. The first approach based on drawing a Tafel-like plot by using the data from the rising part of the current–voltage curve recorded at relatively low scan rates (10 mV s^{-1}) as shown in Fig. 10. The slope of the obtained linear dependence can be used to estimate the value of the symmetry factor (Razmi and Azadbakht, 2005). As can be deduced from Fig. 12, the Tafel slope corresponding to the linear part of the plot was calculated to be about 6.18 (V/decade)$^{-1}$ for substrate **I**a and about 4.1 (V/decade)$^{-1}$ for hydrazone **I**b.

The resulting transfer coefficients assuming one electron per substrate molecule being transferred in the first oxidation step (Table 1) suggest a relatively slow electron transfer.

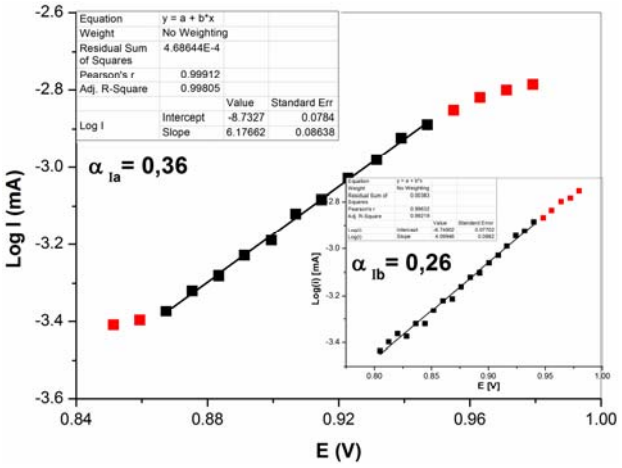

Fig. 12. Tafel-like plot drawn from the rising part of the current-potential curve of compound **I**a recorded in $BMIMBF_4$ at a scan rate of 10 mV s^{-1}. Inset: Same dependence for compound **I**b

An average value of the transfer coefficient can be obtained from the linear regression of the peak potential versus the logarithm of the scan rate (insets of Fig. 8 and Fig. 10) using Eq. (1) (Sauro et al., 2010):

$$E_P = \frac{b}{2}\log v + const. \qquad (1)$$

The dependence of Ep vs. log v has a slope $\partial E_P / \partial \log v$ of 0,068 mV for **I**a and 0.097 mV for **I**b. Note that, as in Eq. (1), the slope of the above dependence is b/2, b being the Tafel parameter. The value of the average transfer coefficients obtained herein is in good agreement to those calculated with the first method (Table 1).

The third method for the estimation of the charge transfer coefficient for an irreversible charge transfer electrode process, like the one studied here, is based on Eq. (2) (Bard and Faulkner, 2001; Wang et al., 2010):

$$\left|E_P - E_{P/2}\right| = \frac{1.857RT}{\alpha n F} \qquad (2)$$

where, E_P represents the peak potential, $E_{P/2}$ is the potential at the half-peak current, α is the symmetry factor, n the number of charges transferred per substrate molecule, R, F and T have their usual meanings.

The average value is found to be 0.127 V for **I**a and 1.34 V for **I**b. The resulting values for α come to confirm the assumption that one electron/molecule is exchanged in the first oxidation step in both substrates.

Table 1. Estimated values for the charge transfer and the diffusion coefficient for **I**a and **I**b in $BMIMBF_4$

Compound[a)]	α_1[b)]	α_{avg}[c)]	α_{app}[d)]	*N (estimated)*	$D / cm^2 s^{-1}$
Ia	0.364	0.434	0.440	1	$9.25 \cdot 10^{-8}$
Ib	0.260	0.303	0.350	1	$8.76 \cdot 10^{-8}$

[a)]Conditions: compound concentration $c=8 \cdot 10^{-3}$ mol·dm^{-3}, ref. Ag/RTIL; [b)] data obtained from the Tafel-like plot; [c)] data obtained from the slope of Ep vs. log v; [d)] data obtained from Eq. (2)

The obtained data shows that the substrates are exhibiting an average value for α of less than 0.5 meaning that the mechanism of the studied electrode process is kinetically controlled by the electron transfer following a stepwise or concerted pathway.

The diffusion coefficient for the studied compounds in $BMIMBF_4$ was estimated from the plot of i_p vs. $v^{1/2}$, which yields a straight line in both cases, as a characteristic of a purely diffusion controlled process at larger overpotentials. The peak current density can be expressed as a function of scan rate (Eq. 3) (Bard and Faulkner, 2001):

$$i_P = 0.496 nFC^* \left(\frac{\alpha nF}{RT} \right)^{1/2} D^{1/2} v^{1/2} \qquad (3)$$

where n is the number of electrons transferred in the first oxidation step, C^* the bulk concentration of the electroactive species, D the diffusion coefficient and v the sweep rate, the other symbols having their usual meaning. Calculating the slope of i_p vs. $v^{1/2}$ and careful conversion of the employed units permitted the estimation of D as shown in Table 1. The values are of two orders of magnitude lower than those obtained for similar compounds in molecular solvents. The difference might appear due to the higher viscosity of the medium or due to ion-pairing effects seen in RTILs.

4. Conclusions

The present study of hydrazones **I**a and **I**b in $BMIMBF_4$ represents, to our knowledge, the first electrochemical data reported for such compounds in RTILs. The voltammograms recorded in the RTIL are fairly similar to those obtained in ACN being characteristic for an oxidation involving two distinct steps (ECEC mechanism) but revealing some notable differences regarding the anodic oxidation of **I**b. When conducting the cyclic voltammetric experiments in $BMIMBF_4$, compound **I**b showed a number of three irreversible anodic peaks, the third signal may be due to the oxidation of the formed pyrazolo-triazole. The obtained voltammetric data for both substrates lead to the assumption that the cation radical intermediate formed after the first charge transfer step undergoes a deprotonation reaction in a subsequent homogenous process implying the BF_4^- anion of the RTIL to form HBF_4. Estimation of the charge transfer coefficient by three distinct methods showed that most probably this phase is indeed governed by a stepwise mechanism and that the charge transfer step occurs relatively slow. Although additional data analysis has to be performed in order to elucidate the details regarding the second charge transfer as well, it is possible to foresee that the mentioned RTIL may be used as an appropriate "green" alternative for performing the anodic cyclization of the studied substrates.

Acknowledgements

The authors would like to thank the International Office at the Vienna University of Technology for funding this research though the programme "*Mitteln zur Förderung von Auslandsbeziehungen*" as well as Univ. Prof. Dipl. Ing. Dr. Ulrich Jordis at the Vienna University of Technology for facilitating this research and Lect. Dr. Ing. Vasile Bercean at the "Politehnica" University of Timişoara for kindly offering the organic substrates discussed in this work.

References

Bailey J., (1977) Synthesis of 1H-pyrazolo[3,2-c]-s-triazoles and derived azamethine dyes, *Journal of the Chemical Society, Perkin Transactions I*, **18**, 2047-2052.

Bailey J., Bowes E., Marr P., (1967), Photographic colour processes, United Kingdom Patent, No. *GB1247493*.

Bansal R., Thota S., (2013), Pyridazin-3(2 H)-ones: the versatile pharmacophore of medicinal significance, *Medical Chemistry Research*, **22**, 2539-2552.

Bard A.J., Faulkner L.R., (2001), *Electrochemical methods: fundamentals and applications*, John Wiley and Sons, New York, 103-105, 235-237.

Barnes E.O., O'Mahony A.M., Aldousb L., Hardacreb C., Compton R.G., (2010), The electrochemical oxidation of catechol and dopamine on platinum in 1-Ethyl-3-methylimidazolium bis(trifluoromethylsulfonyl)imide ([C2mim][NTf2]) and 1-Butyl-3-methylimidazolium tetrafluoroborate ([C4mim][BF4]): Adsorption effects in ionic liquid voltammetry, *Journal of Electroanalytical Chemistry*, **646**, 11-17.

Bercean V., (1988), *Heterocyclic compounds as intermediates for the production of the color photographic materials*, PhD Thesis, Politehnica University of Timişoara, Romania.

Bercean V.N., Badea V., Ilici M., Neda I., Csunderlik C., (2005), The synthesis and characterization of 1H-3-methyl-4-ethoxycarbonyl-5-arylidenhydrazino-pyrazoles, intermediates in the synthesis of 1H-3-aryl-6-methyl-pyrazolo(5,1-c)(1,2,4)-triazoles, *Revista de Chimie*, **56**, 297-301.

Bhat M.A., Ingole P.P., (2012), Evidence for formation of ion pair stabilized diiodomethane radical anion in 1-butyl-3-methylimidazolium tetrafluoroborate room temperature ionic liquid, *Electrochimica Acta*, **72**, 18-22.

Brett C.M.A., Brett O., (1994), *Electrochemistry, Principles, Methods, and Applications*, Oxford University Press, New York.

Brillas E., Siré I., (2011), *Electrochemical Remediation Technologies for Waters Contaminated by Pharmaceutical Residues,* In: *Environmental Chemistry for a Sustainable World,* Lichtfouse E., Schwarzbauer J., Robert D. (Eds.), Springer, Dordrecht Heidelberg London New York, 298-342.

Cekic-Laskovic I., Minic D.M., Baranac-Stojanovic M., Markovic M., Volanschi E., (2009), Cyclic Voltammetry Study of (5_ Ethoxycarbonylmethylidene_ 4_ oxothiazolidin_ 2_ ylidene)_ N_ phenylethanamide, *Russian Journal of Physical Chemistry A*, **83**, 1571-1576.

Costea L.V., Bercean V., Badea V, Ţăranu I., Chiriac A., (2006a), Reactions of 1H-3-methyl-4-ethoxycarbonyl-5-benzylidenehydrazino-pyrazole in nonaqueous media under conditions of undivided and divided-cell electrolysis, *Revista de Chimie*, **57**, 834-837.

Costea L.V., Bercean V., Badea V., Gerdes K., Jordis U., (2006b), Synthesis and electrochemical behavior of some 1H-3-methyl-4- ethoxycarbonyl-5-(benzylidenehydrazino)pyrazoles, *Monatshefte für Chemie/Chemical Monthly*, **137**, 737-744.

Costea L.V., Bercean V., Badea V., Fafilek G., Chiriac A., (2008), Anodic oxidation of some 1H-3-methyl-4-ethoxycarbonyl-5-arilidenhydrazino- pyrazoles: Substitution effects and linear free energy relationships, *Revista de Chimie*, **59**, 691-693.

Costea L.V., Bercean V.N., (2009), Green Chemistry: Electrochemical properties and anodic cyclization of 1H-3-methyl-4-ethoxycarbonyl-5-(4-fluoro-benzylidenehydrazino)-pyrazole in nonaqueous solvents, *Sustainability Science Engineering*, 11th WSEAS International Conference on Sustainability in Science Engineering, Timişoara, Vol.1, 147-152.

Diehl D.R., Mbiya K., Wray C.S., (2000), Photosensitive photographic element, Japan Patent, No. *JP2000194102.*

Doble M., Kruthiventi A.K., (2007), *Green Chemistry and Engineering*, Elsevier Science & Technology Books, Amsterdam.

Fotouhi L., Mosavi M., Heravi M.M., Nematollahi D., (2006), Efficient electrosynthesis of 1,2,4-triazino[3,4-b]-1,3,4-thiadiazine derivatives, *Tetrahedron Letters*, **47**, 8553-8557.

Gösser D.K., (1993), *Cyclic Voltammetry: Simulation and Analysis of Reaction Mechanisms*, VCH, New York.

Hollóczki O., Malberg F., Welton T., Kirchner B., (2014), On the origin of ionicity in ionic liquids. Ion pairing versus charge transfer, *Physical Chemistry Chemical Physics*, **16**, 16880-16890.

Iradyan M.A., Aroyan R.A., Avakimyan D.A., Stepanyan G.M., (2011), Synthesis and antibacterial activity of 2 - hydrazino - 5 - bromomrthyl - 4, 5 - dihydrothiazole hydrazones, *Pharmaceutical Chemistry Journal*, **45**, 26-29.

Kerton F.M., (2009), *Alternative Solvents for Green Chemistry*, The Royal Society of Chemistry, Cambridge.

Lagrost C., Preda L., Volanschi E., Hapiot P., (2005), Heterogeneous electron-transfer kinetics of nitro compounds in room-temperature ionic liquids, *Journal of Electroanalytical Chemistry*, **585**, 1-7.

Laviron E., (1980), A multilayer model for the study of space distributed redox modified electrodes: Part I. Description and discussion of the model, *Journal of Electroanalytical Chemistry and Interfacial Electrochemistry*, **112**, 1-9.

Nicholson R.S., Shain I., (1964), Single scan and cyclic methods, applied to reversible, irreversible and kinetic systems, *Analytical Chemistry*, **36**, 706-723.

Pletcher D., Greff R., Peat R., Peter L.M., (2002), *Instrumental Methods in Electrochemistry*, Horwood Publishing.

Razmi H., Azadbakht A., (2005), Electrochemical characteristics of dopamine oxidation at palladium hexacyanoferrate film, electroless plated on aluminum electrode, *Electrochimica Acta*, **50**, 2193-2201.

Rollas S., Küçükgüzel G., (2007), Biological Activities of Hydrazone Derivatives, *Molecules*, **12**, 1910-1939.

Sauro V., Magri D.C., Pitters J.L., Workentin M.S., (2010), The electrochemical reduction of 1,4-dichloroazoethanes: Reductive elimination of chloride to form aryl azines, *Electrochimica Acta*, **55**, 5584-5591.

Sun P., Armstrong D.W., (2010), Ionic liquids in analytical chemistry, *Analytica Chimica Acta*, **661**, 1-16.

Tatsuo T., Akira O., Yoriko N., Tawara K., (1998), Electrophotographic color toner, Japan Patent, No. *JPH1020559.*

Wagner M., Kvarnström C., Ivaska A., (2010), Room temperature ionic liquids in electrosynthesis and spectroelectrochemical characterization of poly(para-phenylene), *Electrochimica Acta*, **55**, 2527-2535.

Wang D., Chen S., Liu J., Xu C., (2010), Determination of Diffusion Coefficient of Isopropanol in Alkaline Medium using Electrochemical Methods on Pd Electrode, *The Open Electrochemistry Journal*, **2**, 11-14.